Geoderma 438 (2023) 116623

Contents lists available at ScienceDirect

Geoderma

journal homepage: www.elsevier.com/locate/geoderma

Impacts of a hydroinfiltrator rainwater harvesting system on soil moisture regime and groundwater distribution for olive groves in semi-arid Mediterranean regions

Raul Rojano-Cruz [a], Francisco José Martínez-Moreno [b,*], Jesús Galindo-Zaldívar [c,d], Francisco Lamas [e], Lourdes González-Castillo [c], Gabriel Delgado [a], Jesús Párraga [a], Victoriano Ramírez-González [f], Víctor Hugo Durán-Zuazo [g], Belén Cárceles-Rodríguez [g], Juan Manuel Martín-García [a]

[a] Departamento de Edafología y Química Agrícola, Facultad de Farmacia, Universidad de Granada, Campus Cartuja, 18071, Granada, Spain
[b] Departamento de Geodinámica, Estratigrafía y Paleontología, Facultad de Ciencias Geológicas, Universidad Complutense de Madrid, 28040 Madrid, Spain
[c] Departamento de Geodinámica, Facultad de Ciencias, Universidad de Granada, Campus Fuentenueva, 18071, Granada, Spain
[d] Instituto Andaluz de Ciencias de la Tierra, CSIC- Universidad de Granada, 18071, Granada, Spain
[e] Departamento de Ingeniería Civil, Plaza Campo del Príncipe S/N, 18071, Granada, Spain
[f] Departamento de Matemática Aplicada, E.T.S. de Ingeniería de Caminos, Canales y Puertos, Campus Fuentenueva, 18071, Granada, Spain
[g] Instituto Andaluz de Investigación y Formación Agraria y Pesquera (IFAPA), Centro "Camino de Purchil", Camino de Purchil s/n, 18004, Granada, Spain

ARTICLE INFO

Handling Editor: Morgan Cristine L.S.

Keywords:
Vertical mulching
Water catchment
Olive root
Water deficit
Resistivity contrasts

ABSTRACT

Dry periods in semi-arid regions constitute one of the greatest hazardous features that agriculture faces. This study investigates the effects of using a new device called 'Hydroinfiltrator Rainwater Harvesting System (HRHS) on the water balance of soils. It was designed for arid and semi-arid zones affected by long periods of drought punctuated by heavy rainstorms. The new hydroinfiltrator consists of a net-like shell filled mainly with biochar. It is cylindrical in shape, is placed vertically and is half-buried in the soil around the crop tree to facilitate the infiltration of rainwater, irrigation or runoff water deep into the soil. The experimental plot is located in Baena (Córdoba, southern Spain) in an olive grove where the hydroinfiltrator was installed in 90 olive trees while 10 were left as a control group. In the xeric climate (bordering on arid), typical of the region, soils without a hydroinfiltrator have had a low infiltration rate, which reduces the effectiveness of precipitation and significantly increases the risk of water erosion. The effects of infiltration assisted by the device were analysed by simulating a torrential rain in which 600 L of water were passed through the hydroinfiltrator on an olive tree which had been installed 3 years previously. Geophysical methods (electrical resistivity tomography, ERT), direct analyses of soil samples, both *in situ* and in the laboratory, and theoretical flow models indicated a very significant increase in soil moisture (which nearly tripled in respect to the control group) because water was absorbed into the soil quickly, preventing runoff and water erosion. The soil moisture at 20 cm depth was 2.97 times higher with the HRHS than in the control plots. In addition, olive production increased by 211% and was higher in fat yield by 177%. Moreover, the resistivity profiles, taken by ERT showed that the water that entered the soil accumulated in the root zone of the olive tree, encouraged by the preferential pathways created by the roots and away from the surface, which prevented rapid evaporation during the high temperatures of spring and summer. Here we show for the first time that the use of the hydroinfiltrator rainwater harvesting system represents a significant improvement in the use of scarce water resources caused by climate change, providing agronomic and environmental benefits for rainfed, Mediterranean agricultural systems.

* Corresponding author.
E-mail address: fjmmoreno@ucm.es (F.J. Martínez-Moreno).

https://doi.org/10.1016/j.geoderma.2023.116623
Received 3 March 2023; Received in revised form 3 July 2023; Accepted 28 July 2023
Available online 1 August 2023

1. Introduction

According to future climate change projections, the Mediterranean basins may be particularly vulnerable to drought. (Giorgi and Lionello, 2008). This is due to the fact that they are in the transition zone between an arid climate and a temperate and rainy climate, making them very vulnerable to small changes in the general atmospheric circulation. The expected impacts of climate change in the Mediterranean are: (i) increase in air temperature, (ii) decrease in total annual precipitation, (iii) changes in the seasonal distribution of precipitation with greater inter-annual variability, and (iv) increase in the frequency and intensity of extreme events - droughts, floods, heat waves (Goubanova and Li, 2007). In this sense, several studies showed a trend towards reduced water availability (García-Ruiz et al., 2011) and more extreme and frequent droughts (Hoerling et al., 2012), which will lead to water stress for crops in the future –especially in rainfed cropping systems– and to significant yield losses (Funes et al., 2021; Valverde et al., 2015).

Currently, water resources are overused in most of the Mediterranean, with consumption exceeding water availability. According to Iglesias et al. (2007), water scarcity is one of the major threats in the region. That is, the implementation of deficit irrigation methods as a sustainable adaptation strategy to climate change is considered to be a key factor (El-Nashar and Elyamany, 2023).

Conventional tillage systems lead to encrustation of the soil and the formation of compacted layers, which hinder the infiltration of precipitation and cause significant runoff during heavy rains (Palese et al., 2014). Soil management that allows increasing the availability of water in the soil is the best strategy to improve the productivity of rainfed crops (Delgado et al., 2013; Kumar et al., 2019). In light of this, it is vital to emphasize that the sustainability of rainfed agriculture will largely depend on optimizing water management practices and maintaining soil quality. Particularly, when it comes to the maintenance of rainfed olive (*Olea europea* L.) production, soil conservation practises such as mulching, no-till and/or cover crops that increase infiltration, reduce evaporation and increase water storage in the soil need to be adopted (Durán Zuazo et al., 2009; Palese et al., 2014).

Rainwater harvesting in agriculture can be defined as any type of device or technique that collects, stores and/or increases the availability of rainwater runoff for subsequent productive use, especially in cropping systems (FAO, 2014). There are many examples of the use of water harvesting since ancient times in the Mediterranean region (Beckers et al., 2013). This is an effective strategy to reduce the negative impacts of runoff and increase soil moisture storage through infiltration (Al-Seekh and Mohammad, 2009).

There are numerous studies demonstrating the benefits of using water harvesting systems on rainfed woody fruit trees in arid and semi-arid regions. In this sense, Tubeileh et al. (2009) showed that the use of micro-catchment water harvesting systems in a young olive orchard in Syria increased soil moisture and improved stomatal conductance, leaf water content, leaf nitrogen content and olive tree stem growth. Water harvesting allowed an increase in soil moisture in spring and early summer, the critical times for olive production (Tubeileh et al., 2016). In a study by Tadros et al. (2021) the combination of water harvesting techniques demonstrated that (mulching × microharvesting) significantly improved soil water content, plant morphology and physiology of young rainfed pistachio orchards. Water harvesting systems (half-moon or full moon) combined with mulches (organic or plastic) improved vegetative growth, fruit yield and soil moisture content of apples under rainfed conditions (Kumar et al., 2013). Zhang et al. (2021) estimated that rainwater harvesting in orchards in northwest China increased soil water retention by 13.7% and increased apple yield by 19.1%.

The olive tree is of great socio-economic importance in the Mediterranean region (Fraga et al., 2021). The olive tree is a sclerophyllous species adapted to the semi-arid Mediterranean climate, as it can also grow in dry conditions (Fereres, 1984; Fernández et al., 1997). The species has developed several tolerance mechanisms that enable its adaptability to drought (Connor and Fereres, 2004). However, there is a threshold, estimated at 200 mm per year, below which production declines drastically (Bongi and Palliotti, 1994). For rainfed olive trees, the combined effects of temperature increase and precipitation decrease, will reduce the amount of water available in the soil and exacerbate water stress conditions, making it unlikely that they would be grown in the future in the southern and eastern Mediterranean regions (Tanasijevic et al., 2014).

We present here a new system of rainwater harvesting with the hydroinfiltrator, tested on olive trees in a semi-arid region of Spain affected by long dry periods and intense rainfall. This study aims to evaluate the impact of this new rainwater harvesting system in the Mediterranean environment affected by climate change, through geophysical and soil sampling methods.

2. Material and methods

2.1. Settings – Experimental plot

The study is located in Baena (Córdoba, southern Spain) in the '*La Agusadera*' area with 100 olive trees (Fig. 1). The area consists of Neogene (lower to middle Miocene) and Quaternary deposits belonging to the External Zones of the Betic Cordillera. The principal material of the soils in this area consists of calcareous marl. The topography is irregular; the slopes are east-facing and have an average slope of 7%. The slope is used to create a micro-basin system (64 m^2) around each olive tree, where the water is channeled through two furrows (ridges) into an endorheic micro-catchment of about 0.5 m^2 in area and 0.2 m deep, located about 0.7 m above the trunk of the olive tree. The climate is Mediterranean, with long dry periods and sudden rains in autumn and spring. The mean annual temperature is around 17.5 °C and the total annual rainfall is 450 mm (average, period 2000–2020, Junta de Andalucía, 2022).

The land is devoted to the cultivation of olive trees (variety '*Picuda*') for more than 100 years. The plantation frame is 64 m^2 (8 × 8 m) with an approximate density of 150 olive trees per ha^{-1}. Currently, the olive trees are grown dry and without tillage, using contact herbicides that favour the development of a moss layer (Slate et al., 2023).

At the end of the season, the olive yield (kg per $tree^{-1}$) was measured and fruits from field treatments were sampled to determine fat content, the Soxhlet technique was used and the results were calculated and expressed in percentage of dry weight. (w/w) (Jiménez et al., 2000).

Table 1 displays the main soil characteristics of the experimental hillslope plot used in this study. The clayey loamy soil is made up of Haplic Calcisol (hypercalcic, ochric) (IUSS Working Group WRB, 2014) with an Ap-B-Ck-Ckm-C'k profile (Fig. 2). The pH is basic (between 8.3 and 8.6), with a high content of equivalent calcium carbonate (≥38%). The structure changes from subangular blocks (Ck) to massive (C'k) measuring 49 cm. The porosity is suitable for cultivated soil, especially in horizons B and Ck where there are more fine pores. The first 41 cm (horizons Ap and B) show the greatest richness of olive roots; below 49 cm (upper limit of the Ckm horizon), no more olive roots were detected. This limitation of roots to 49 cm in the profile described (in the middle between two rows of olive trees) is caused by the presence of a thin calcareous crust between 49 and 51 cm (Ckm horizon), which acts as a barrier for roots and to water infiltration.

2.2. Hydroinfiltrator rainwater harvesting system (HRHS)

The new *HRHS* (Delgado et al., 2019; ES Patent No.: ES2793448 B2) consists of a mesh-like shell filled mainly with biochar. It has a cylindrical shape with a maximum dimension of 50 cm and a diameter of 30 cm (Fig. 3), it is placed vertical and half-buried in a pit ~ 0.5 m above the trunk of the crop tree –so that about 10 cm protrude above the surface of the pit to avoid having sediments clog the system– it greatly facilitates the infiltration of rainwater, irrigation or runoff water into the

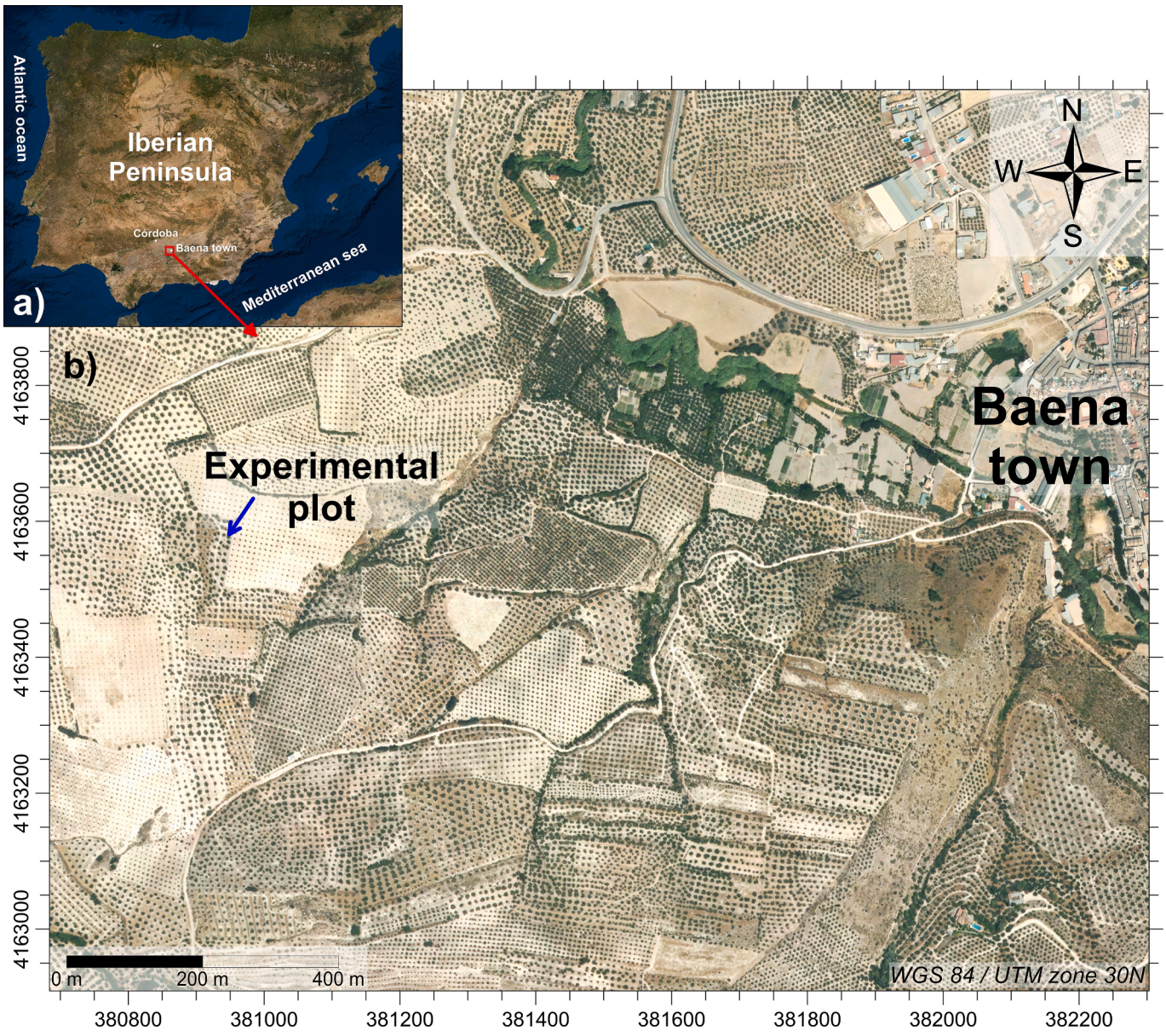

Fig. 1. Location of the experimental plot (a) in the south of the Iberian Peninsula, (b) in the La Agusadera area, near Baena town (Córdoba, S Spain).

depth (avoiding evaporation).

In 2016, a *HRHS* was installed in each micro-basin for 90 olive trees on the experimental plot. No devices were placed in the micro-basins of the remaining 10 olive trees (the control group).

2.3. Numerical flow model

A numerical stress–strain model was developed to simulate the flow processes and drainage network triggered by the *HRHS* and the response of the soil. This takes into account a water flow that is directed through the *HRHS*, which uses gravity to penetrate the soil. The modelling was carried out using Phase2 software (Rock Science), considering a uniform discharge P (m s^{-1}) and the characteristics of the soil medium (Fig. 2); the olive tree was modelled as a load absorbed in the middle of the area of 1 m^2, with a weight of 3 tons; the area of influence of the roots was modelled with a curved surface of 5 m in diameter and a depth of 0.8 m; the *HRHS* was designed to be a perfect philtre, completely permeable and confined. Finally, a flow rate of 1200 L h^{-1} m^{-2} was calculated. The study profile covers an area of 10 × 10 m and a depth of 10 m, which is considered sufficient to cover the area affected by the infiltration and to reach a steady state of the potential flow network without being affected by the boundary conditions and around the olive tree. The filtration analysis and the modelling of the drainage network were carried out using the finite element method. Triangular elements with 6 vibration nodes were used, they were refined in the areas with the greatest variability, and used an unconstrained model for the meshing.

2.4. Direct measurements of water infiltration and soil moisture

Soil infiltration rates were measured in the field using the double ring method as indicated by Li et al. (2019). Due to water scarcity in the area and the difficulty in accessing the experimental site, an inner ring with a diameter of 25 cm and an outer ring with a diameter of 33.3 cm were used, with a ratio of inner to outer diameter of 1.33, as indicated by the cited authors. The height of the rings was 50 cm and they were driven about 10 cm into the ground. The experiment was conducted in August 2020 in order to ensure initial dryness of the soil and to establish flow in an unsaturated medium. The infiltration rate was studied in 5 areas with *HRHS* installed and 5 without them (control areas). In the second case, the height of the water column was about 40 cm and they

Table 1
Main soil properties of the experimental plot used in this study.

	Ap	B	Ck	Ckm	C'k
Depth (cm)	0–22	22–41	41–49	49–51	>51
Texture	cl	cl	cl	nd	cl
Structure	m2sbk	m2sbk	m2sbk	m	m
Moist colour (Munsell)	10YR 6/2	10YR 5/2	10YR 7/2	10YR 8/2	10YR 8/4
Porosity	1mp, 1fp, 3vfp	1mp, 2fp, 2vfp	1mp, 2fp, 2vfp	0	1mp, 1fp, 0vfp
Roots	2fr, 2vfr	2fr, 2vfr	1mr, 1fr, 1vfr	0	0
Sand (%)	16.1	11.6	16.6	nd	22.4
Clay (%)	43.8	34.1	29.5	nd	14.5
Silt (%)	40.1	54.3	53.9	nd	63.1
W33 (%)	31.90	33.69	34.18	nd	37.28
W1500 (%)	15.74	17.25	16.82	nd	12.06
AW (mm cm^{-1})	2.36	2.43	2.6	nd	3.89
$pH_{(H2O;\ 1:1)}$	8.3	8.4	8.5	nd	8.6
SOC (%)	1.26	0.83	0.75	nd	0.30
$CaCO_3$ eq. (%)	38.0	41.8	48.6	78.3	45.0
EC (dS m^{-1})	0.46	0.37	0.37	nd	0.37

Abbreviations: nd = no determined. **Texture** class: cl = clay loam. **Structure**: Size: m = medium; Grade: 2 = moderate; Type: sbk = subangular blocks; m = massive. **Porosity**: Quantity: 0 = none, 1 = few, 2 = common, 3 = many; Size class: vfp = very fine, fp = fine, mp = medium. **Roots**: Quantity: 0 = none, 1 = few, 2 = common; Size class: vfr = very fine, fr = fine, mr = medium. W33 = Water retention at 33 kPa; W1500 = Water retention at 1500 kPa; AW = available water; SOC = soil organic carbon; $CaCO_3$ eq = calcium carbonate equivalent; EC = electrical conductivity.

were measured in one hour. In the first case, the inner ring was directly above the device. It was not possible in any of the cases to keep the water column constant at this point given the high infiltration rate, so these measurements are estimates. Due to the limited capacity of the water tank transported to the experimental site (600 L), it was not possible to run the infiltration experiment for one hour.

All moisture measurements of the soil samples were carried out in the laboratory using gravimetry. Soil moisture was monitored by estimating it every month (around the 15th of every month) between September 2017 and December 2022. Samples were taken at a depth of 20 cm with an Eijkelkamp undisturbed soil drill, both in the control plots (10) and in the experimental plots (10).

Finally, the water balance was estimated with average values for precipitation, temperature and potential evapotranspiration of the Baena meteorological station (years 2000 to 2022) provided by the *Junta* de Andalucía (2022) and taking into account the available water reserve in the soil (obtained from the values of AW, Table 1). Therefore, a monthly soil water balance was established (Soil Survey Staff, 1999) taking into account the parameters of reserve status, reserve variation, actual evapotranspiration (RET), surplus and deficit.

2.5. *Electrical resistivity tomography - ERT*

Electrical methods in geophysics determine the resistivity distribution at depth. This makes it possible to measure changes in moisture and water content from the surface down to a depth of several hundred metres (Martínez-Moreno et al., 2015). This technique is used, for example, in agriculture, in determining the groundwater level, in aquifers and in structural geology, among others (Martínez-Martos et al., 2017; Martos-Rosillo et al., 2019).

Electrical resistivity tomography (ERT) calculates the resistivity distribution in the subsurface by installing steel electrodes with a constant spacing along a line. Electrical current is injected through selected pairs of electrodes and differential potential measures are done through other pairs of electrodes. The different combinations of electrode pairs determine the different protocols to develop the measurements. Two perpendicular transects were made in an olive tree –horizontal and at

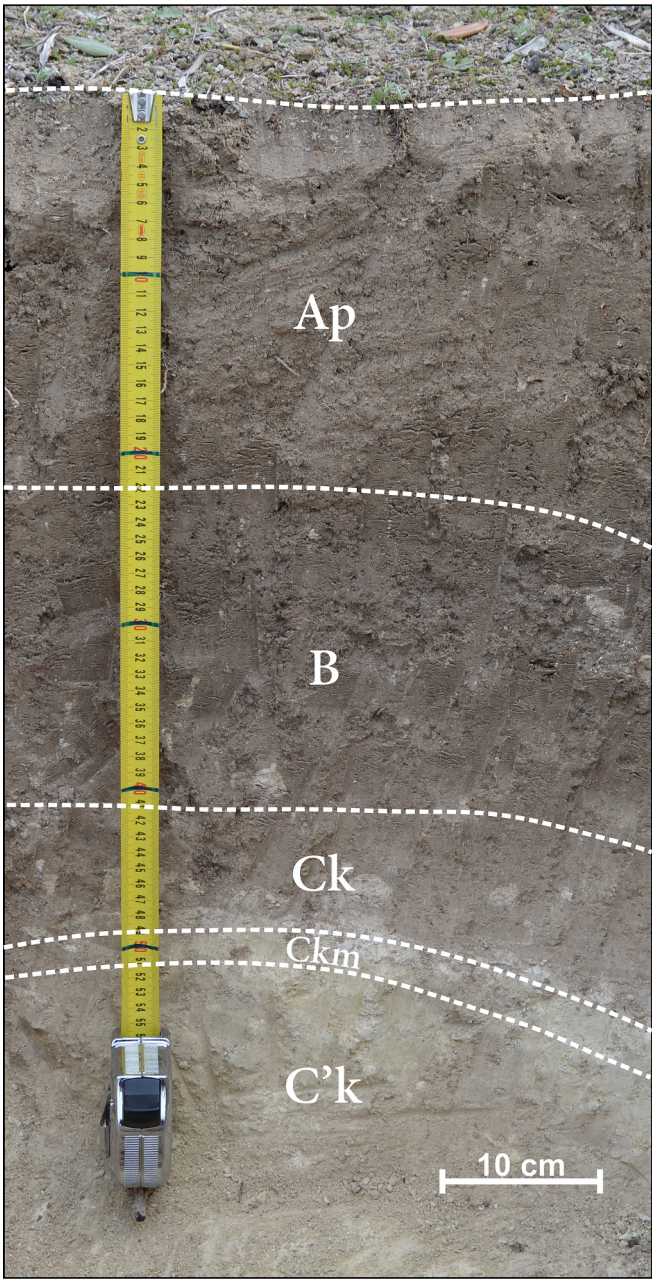

Fig. 2. Characteristic of soil profile of the experimental plot, showing a vertical section of the soil with the main horizons (Ap, B, Ck, Ckm, and C'k).

maximum slope– centred on the *HRHS*, using the ABEM Terramenter SAS4000 instrument. Both profiles have an electrode spacing of 0.1 m and are 8 m long. They were acquired with a multi-channel gradient electrode array. The gradient protocol uses the Wenner-Schlumberger configuration adapted to multi-channel resistivity measurement systems.

Both profiles were recorded in time-lapse under two different moisture conditions on the same day: first, before a simulated rainfall under the driest soil conditions (August 2020), and second, after a simulation of the rainfall with the addition of 600 L of water. Some fertilisers were added to the water to increase the resistivity contrasts.

Data inversion was performed with Res2Dinv software (v.3.59; Geotomo Inc.) using the standard least squares method and model refinement constraint due to the larger amount of data (Loke, 2022). Other parameters used were as follows: a mesh made up of model cells, 4 nodes per unit electrode spacing, an initial factor of 0.3 which reduces

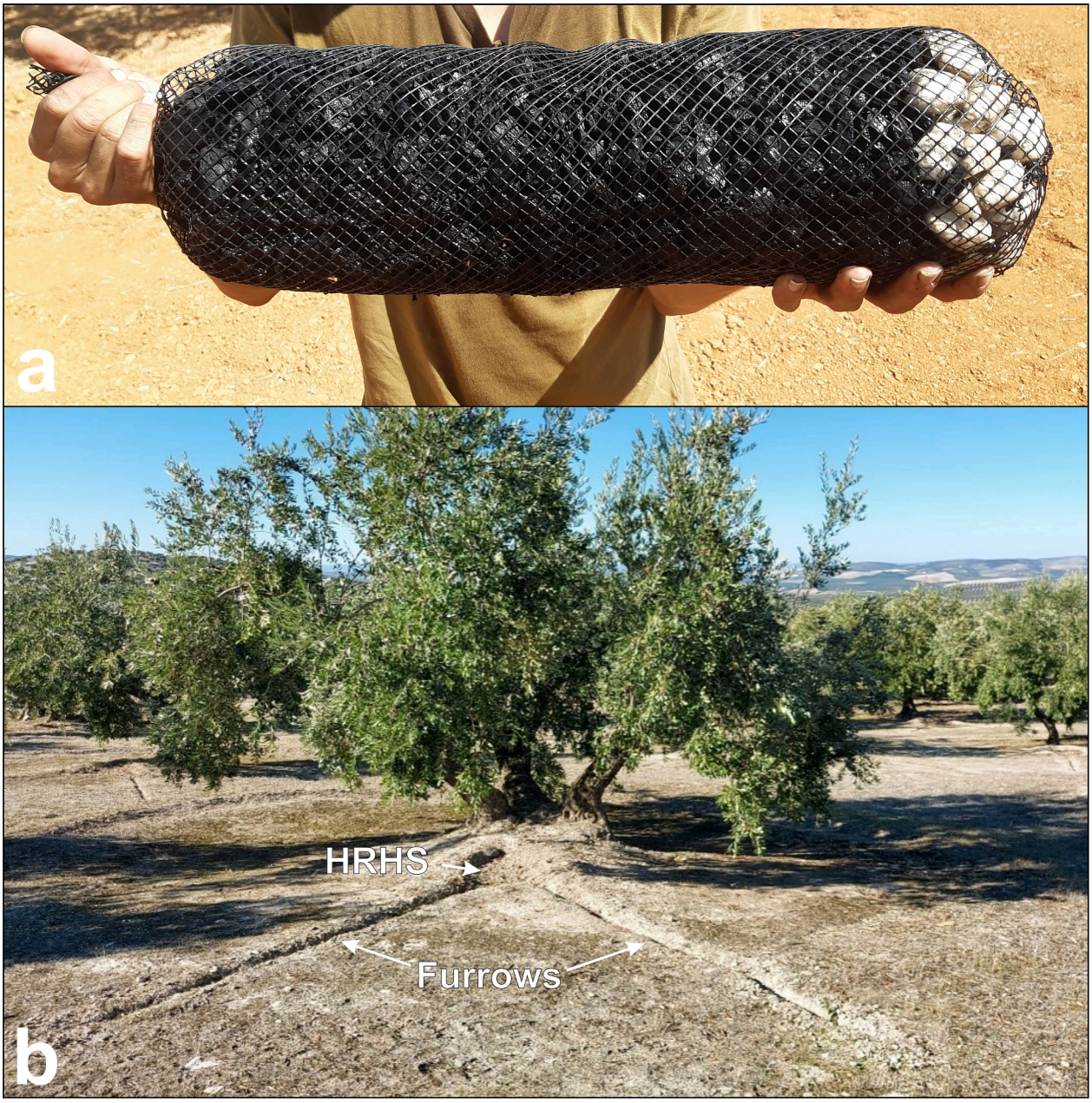

Fig. 3. Hydroinfiltrator Rainwater Harvesting System (HRHS). a) General aspect of the HRHS. b) Field installation close to the olive trunk with two furrows for collecting rainfall and surface runoff.

the effect of side blocks, and finite elements with trapezoidal elements. As the profiles were acquired in time-lapse with moisture changes, it was possible to calculate the percentage moisture changes using the software Res2Dinv.

3. Results

3.1. Hydrological parameters

The amount of water infiltrated into the soil through the *HRHS* was about 600 L –capacity of the water tank– in about 30 min, so the calculated infiltration rate was 1200 L h^{-1}. In the five control plots (without *HRHS*), the measured infiltration rates were 23, 31, 34, 42 and 45 L h^{-1} (mean 35 ± 8.8 L h^{-1}). This demonstrates an increase in the infiltration rate of 3429% when using the *HRHS*.

In contrast, soil moisture at 20 cm depth follows a seasonal cycle, decreasing in the summer months and increasing in the winter ones (Fig. 4). Moisture is always higher in the olive trees with the *HRHS* than in the control trees, and these differences are magnified in the winter months by a cumulative effect of water. As for the rainfall line, the soil moisture line of the control samples follows a more similar pattern than this of the *HRHS*. For the mean values (months of 2018–22; n = 48), the soil moisture at 20 cm depth was 2.97 times higher in the plots with the *HRHS* than in the control plots.

Based on the previous results, we can compare the water balances for the control soils and the soils with the *HRHS* (Fig. 5). For the soil with the *HRHS*, and according to Fig. 4, we assume that 2.97 times more rainwater infiltrates the soil than in the soil around the control group. In this way, the implantation of the system leads to a drastic change in the moisture regime in the soil, because: (a) the water deficit and duration are reduced from 842 L m^{-2} yr^{-1} and 6.5 months duration in the control group soil to 554 L m^{-2} yr^{-1} and 3.5 months duration in the soil with the

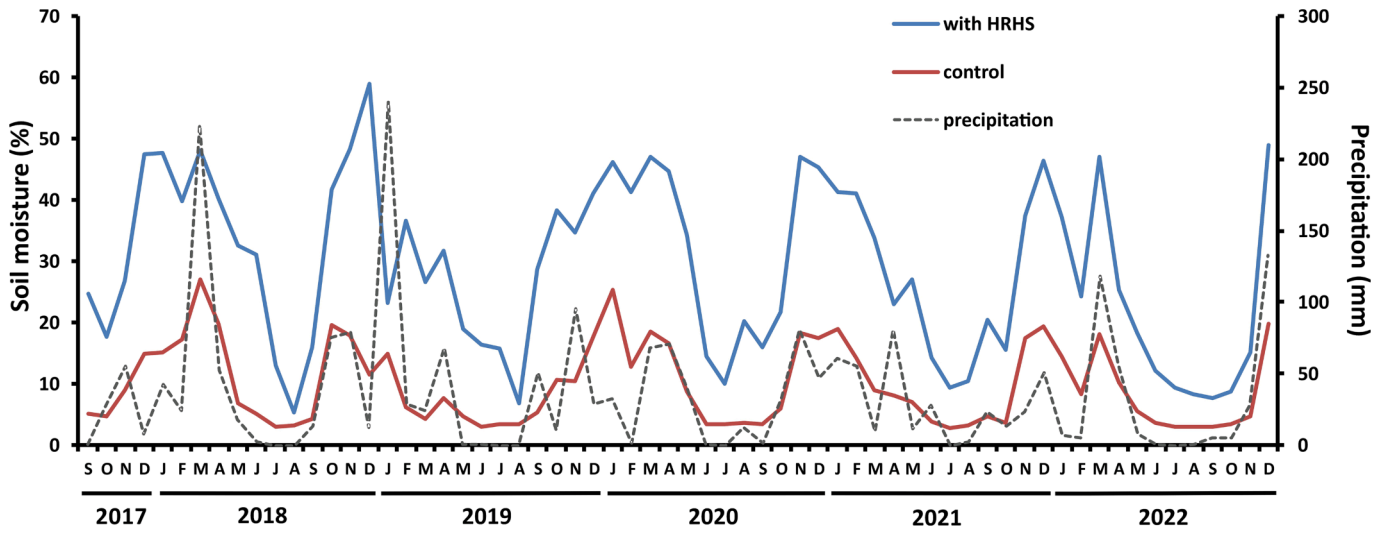

Fig. 4. Variation in monthly precipitation and soil moisture in areas with and without HRHS at 20 cm soil depth (and 20 cm from HRHS, if applicable) during 2017–22.

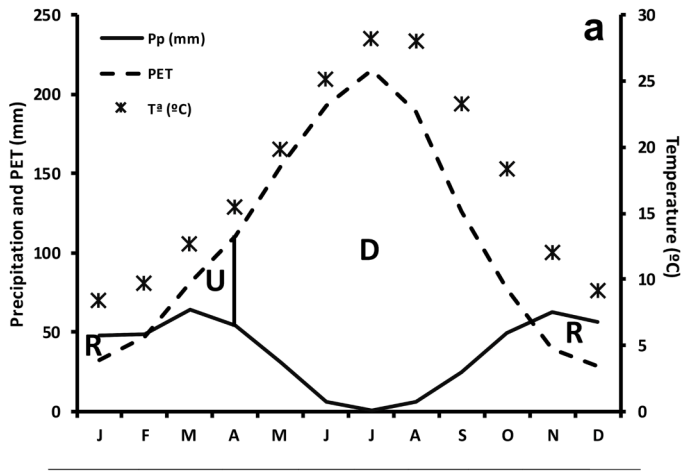

	Tª (ºC)	Pp (mm)	PET	WRV	WR	AET	EW	WD
January	8.4	48.0	32.3	39.3	**66.7**	**32.3**	**0.0**	**0.0**
February	9.7	48.6	47.1	1.5	**68.2**	**47.1**	**0.0**	**0.0**
March	12.6	64.1	81.0	-16.9	**51.3**	**81.0**	**0.0**	**0.0**
April	15.5	54.5	110.7	-51.3	**0.0**	**105.8**	**0.0**	**4.9**
May	19.8	30.9	154.5	0.0	**0.0**	**30.9**	**0.0**	**123.6**
June	25.1	6.2	193.0	0.0	**0.0**	**6.2**	**0.0**	**186.8**
July	28.2	1.0	215.1	0.0	**0.0**	**1.0**	**0.0**	**214.1**
August	28.0	6.0	189.0	0.0	**0.0**	**6.0**	**0.0**	**183.0**
September	23.3	24.6	125.9	0.0	**0.0**	**24.6**	**0.0**	**101.3**
October	18.3	49.3	77.7	0.0	**0.0**	**49.3**	**0.0**	**28.4**
November	12.0	62.9	39.6	23.3	**23.3**	**39.6**	**0.0**	**0.0**
December	9.1	56.4	28.7	27.7	**51.0**	**28.7**	**0.0**	**0.0**
Total/mean	17.5	452.5	1294.7			452.5	0.0	842.1

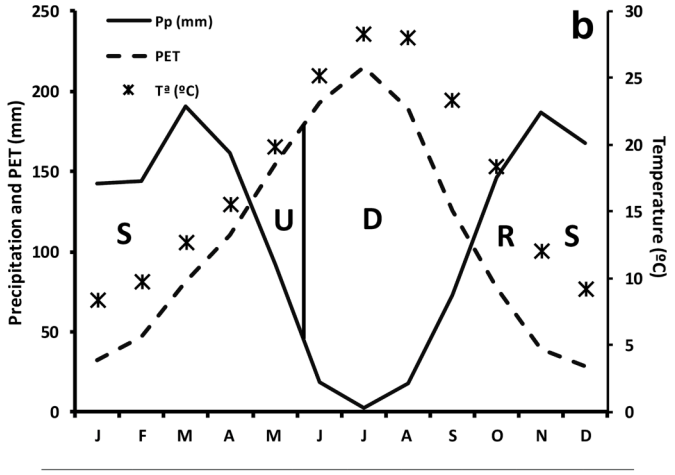

	Tª (ºC)	Pp (mm)	PET	WRV	WR	AET	EW	WD
January	8.4	142.6	32.3	0.0	**119.0**	**32.3**	**110.3**	**0.0**
February	9.7	144.2	47.1	0.0	**119.0**	**47.1**	**97.1**	**0.0**
March	12.6	190.4	81.0	0.0	**119.0**	**81.0**	**109.4**	**0.0**
April	15.5	161.7	110.7	0.0	**119.0**	**110.7**	**51.0**	**0.0**
May	19.8	91.9	154.5	-62.6	**56.4**	**154.5**	**0.0**	**0.0**
June	25.1	18.5	193.0	-56.4	**0.0**	**74.9**	**0.0**	**118.1**
July	28.2	2.9	215.1	0.0	**0.0**	**2.9**	**0.0**	**212.2**
August	28.0	17.9	189.0	0.0	**0.0**	**17.9**	**0.0**	**171.1**
September	23.3	73.0	125.9	0.0	**0.0**	**73.0**	**0.0**	**52.9**
October	18.3	146.5	77.7	68.8	**68.8**	**77.7**	**0.0**	**0.0**
November	12.0	186.9	39.6	50.2	**119.0**	**39.6**	**97.1**	**0.0**
December	9.1	167.5	28.7	0.0	**119.0**	**28.7**	**138.8**	**0.0**
Total/mean	17.5	1344.0	1294.7			740.3	603.7	554.3

Fig. 5. Soil water balance based on mean values between 2000 and 2022: a) soil without HRHS (control soil); b) soil with HRHS. Pp (mm): precipitation; PET: potential evapotranspiration; R: recharge; U: use; D: deficit; S: surplus; AET: Actual Evapotranspiration; WRV: Water Reserve Variation; WR: Water Reserve; EW: Excess of water; WD: Water deficit.

HRHS; (b) the soil's water reserve is not replenished in the control group soil (it is in the soil with the *HRHS* system); (c) the actual evapotranspiration is greater in the soil with the *HRHS* (740 L m^{-2} yr^{-1}) than in the control soil (453 L m^{-2} yr^{-1}), which translates into higher production because the olive tree has a greater water volume (Lorite et al., 2018); d) there is an excess of water in the soil with the *HRHS* (604 L m^{-2} yr^{-1}; 0 L m^{-2} yr^{-1} in the control group soil), which, being infiltrated water, means a return flow of water to the basin.

For both treatments, control group soil and soil with *HRHS*, the temperature regime is thermic and the moisture regime is xeric (Soil Survey Staff, 2014), with the moisture regime in the control soil being drier. Therefore, a micro-edaphoclimate, which could be described as an *island of moisture*, is created in the soils with the *HRHS* devices.

3.2. Theorical flow model

As a result of the filtration analysis and the modelling of the drainage network with the finite element method shows the theoretical lines of

the filtration flows (Fig. 6). This theoretical model, calculated on a standard site, with the characteristics of the olive microbasins analysed, shows that the seepage flows mainly demonstrate gravitational behaviour originating from the hydroinfiltrator, with minimal lateral extension in depth. This behaviour of the vertical flows occurs because the model takes into account that the hydroinfiltrator penetrates the most impermeable calcareous crust (horizont Ckm) and reaches the marls substrate (horizont C'k).

3.3. Resistivity profiles

The ERT profiles are shown in Fig. 7. Prior to rain simulation, both profiles show resistivities between 50 and 200 O*m (Ωm), with small concentrated areas of high resistivity (~500 Ωm) indicating compacted and dry zones, and punctuated small areas of low resistivity (~20 Ωm) indicating the presence of clay or higher moisture (Fig. 7a and 7c). The position of the olive tree and the *HRHS* are identified as zones of high resistivity (greater than650 Ωm).

After rain simulation, water infiltration and distribution are highlighted by areas of low resistivity (~5 Ωm) extending from the surface to 1 m depth (Fig. 7c and 7d). In profile 1, the water infiltration extends over a length of 2 to 7 m in the profile. In profile 2, this area is between 3 and 6 m long. At metre 5.6 of profile 2, the low resistivity at the bottom indicates that the infiltrated water goes deeper. However, this could also be a side effect of the method (Loke, 2022), thus we cannot assume that the water infiltrates deeper in this area.

The 3D view of the profiles shows the spatial distribution of the water infiltration in the ground (Fig. 8a). The low resistivity (blue colours) indicates the presence of water infiltration with stronger concentration in the NE-SW direction, following the general slope of the area. The time-lapse allows us to calculate the moisture content change in percentage after the rain simulation (Fig. 8b). The profiles show a change of 100% in the moisture of the soil in the area around the root, which acts as preferential pathways of water.

3.4. Effects of the HRHS on olive production

Increasing the amount of water infiltrated by the device leads to a greater increase in the production and fat yield of the olives (Fig. 9). On the experimental plot, production was monitored from 2017 to 2022 seasons. The olive yield where the device was installed increased by 211% and fat yield by 177%. In general, the olive trees with the infiltration devices produced on average 373% more oil than the olive trees without the HRHS. It is widely accepted that rainfed conditions are associated with less-productive farms with limited profitability because of the crown growth and alternate bearing, being markedly dependent on rainfall (Rodrigo-Comino et al., 2021). The findings of the present experiment are in line with many studies that have reported the positive

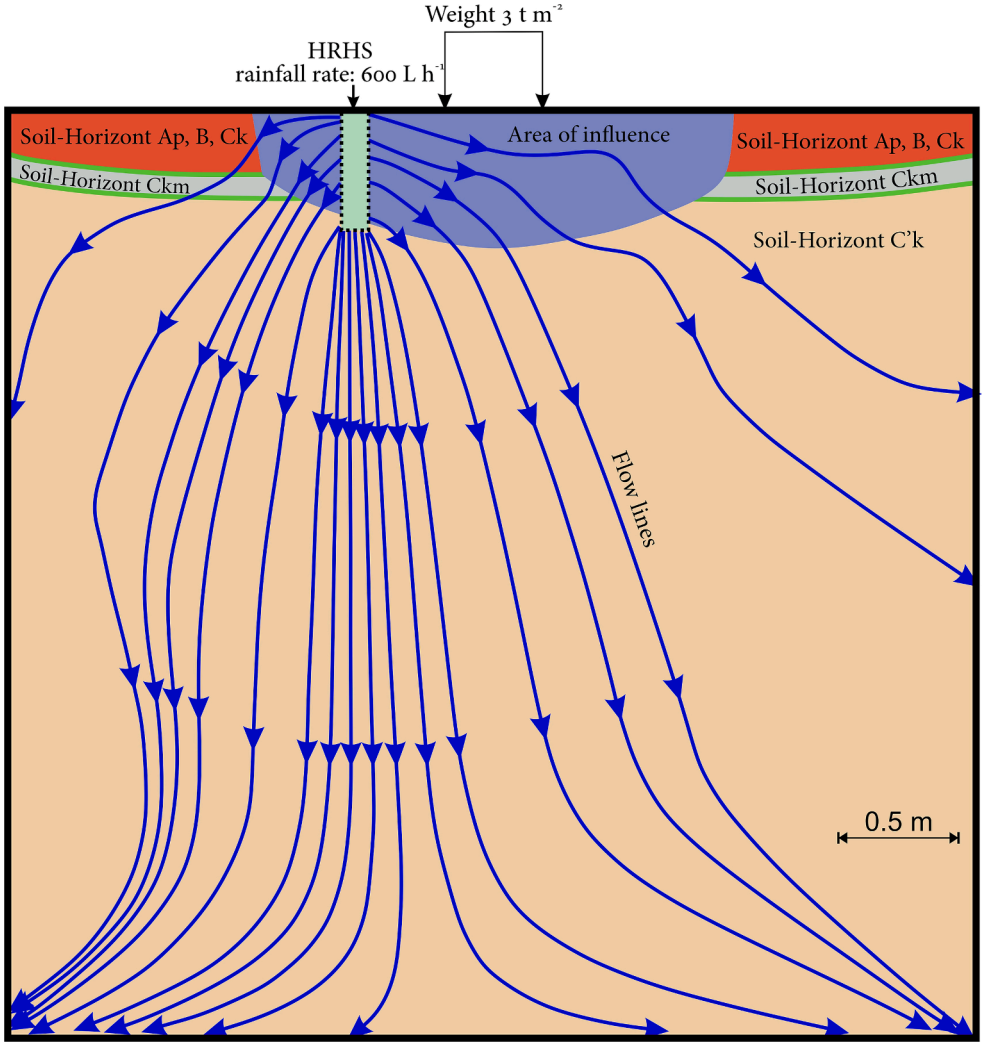

Fig. 6. Numerical flow model showing the theoretical lines of filtration flows with gravitational behaviour from the hydroinfiltrator after rain simulation of 600 L h^{-1}.

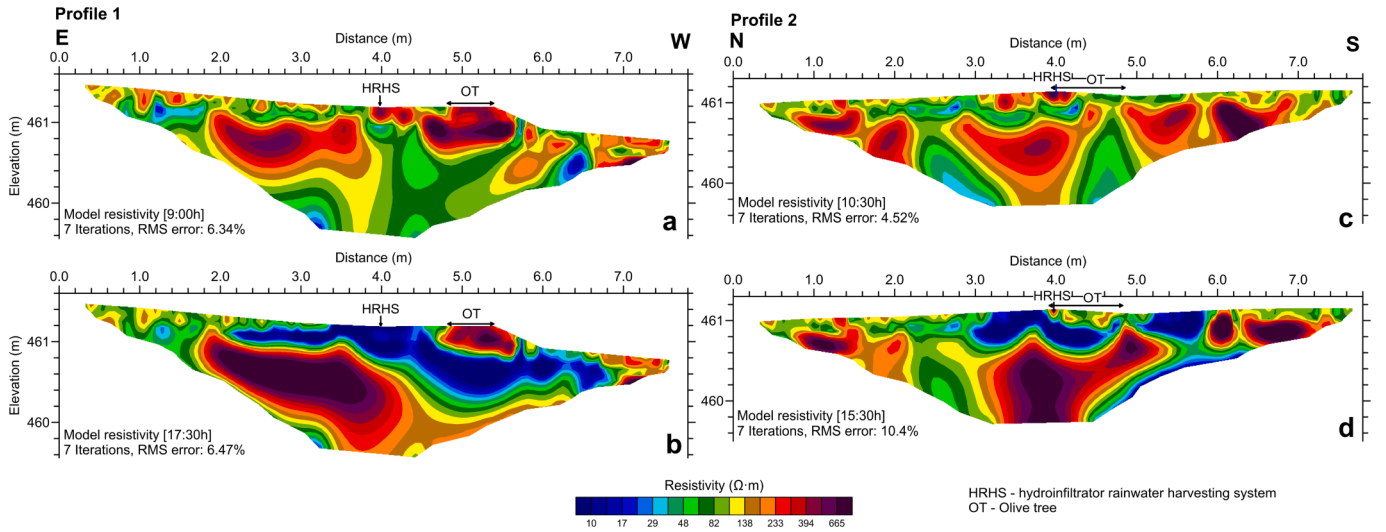

Fig. 7. Electrical Resistivity Tomography (ERT) profiles measured in perpendicular directions before (top, models a and c) and after (bottom, models b and d) the rainfall simulation. The positions of the HRHS and the olive tree (OT) are indicated, as well as the hour it was recorded.

impact of supplementary water on olive yield for Mediterranean environments (Inglese et al., 1996; Costagli et al., 2003; Lodolini et al., 2016; Freihat et al., 2021). That is, our results suggest an improvement in the productivity of the trees receiving rainfall water, resulting in an increase in olive yield, avoiding the loss by runoff and evaporation from the surface of the soil.

On the other hand, the fat content (and its composition) is an essential parameter in determining the quality and authenticity of olive oil. These results can give useful indications for explaining the relationship between olive rainfed orchards with and without *HRHS* system based on the optimization of the use of rainfall water and its positive implications on olive oil quality. The data found in the present experiment agree with those, which reported the effects of water on olive oil quality (Gómez et al., 2007; El Riachy et al., 2017; Trabelsi et al., 2022).

4. Discussion

4.1. Available water and soil water balance

Based on the available water in the soil (Table 1), the water reserve in the first 49 cm of the layer thickness –where the olive roots were described– is estimated to be 120 mm. By extrapolating the data, it is estimated that each micro-basin (64 m^2) can retain 7.68 m^3 of usable water reserves (1200 m^3 on one hectare).

In the water balance model (Fig. 5), the soils with the *HRHS* complete the recharge of the reserve on November 10th, while the control soils never do so. The results of the soil moisture measurement confirm these calculations, as it is higher and lasts longer in the soils with the *HRHS* (Fig. 4). Once the reserve in the soils with the *HRHS* is used up, the excess water can be expected to percolate towards the water table, which the calculations estimate at 90.6 $m^3\ ha^{-1}\ yr^{-1}$. This would help to reduce pressure on water resources and mitigate the threat of water scarcity which will be one of the greatest challenges facing humanity in the coming decades (Gosling and Arnell, 2016). Thus, the *HRHS* system improves soil moisture availability, particularly under low-rainfall conditions and could encourage the maintenance of crop yield in a changing climate scenario in the Mediterranean region (Iglesias et al., 2007). In areas where there is a water deficit, the aim of *HRHS* is to increase water storage in the soil and reduce evaporation and surface runoff (Al-Seekh and Mohammad, 2009; Abhilash Joseph et al., 2020). Soil water balance data showed that the *HRHS* is a promising strategy for soil water harvesting by intercepting the rainfall and surface runoff (Fig. 5).

Additionally, the infiltration of water directly into the subsoil through the *HRHS* reduces the soil erosion due to water runoff. This fact was confirmed in the experimental plot, where no signs of water erosion, such as furrows or gullies were observed close to olive with *HRHS*. The issue of water erosion is extremely important because an increase in high-intensity rainfalls in the Mediterranean semi-arid areas is expected. The implementation of sustainable strategies is urgent in order to mitigate the effects of water erosion exacerbated by climate change, especially for hillslope farming with woody rainfed crops (Cárceles Rodríguez et al., 2021; Ferreira et al., 2022).

4.2. The role of olive roots as preferential pathways and groundwater distribution

The distribution of water in the soil as determined by ERT could be due to the preferential pathways of water (Weil and Brady, 2017) (Figs. 6, 7, and 8b). In the case studied, these preferred pathways are generated by the development and distribution of olive roots in the Mediterranean climate and are conditioned by the morphological and physical properties of the soil.

The roots of olive trees are adapted to the Mediterranean climate and tend to distribute themselves in the shallow part of the soil to make better use of the scarce and at times, torrential rainfall, and nutrients derived from the decomposition by microorganisms of the plant debris (twigs and leaves) that fall on the surface (Deng et al., 2017). The highest root densities are in the first 60 cm of the soil with the majority in the top layers, usually within the first 40 cm (Masmoudi-Charfi et al., 2011; Deng et al., 2017). In the distribution of the different levels of the olive tree roots, Sorgonà et al. (2018) found a maximum between 45 and 60 cm for the roots of the first order, another between 30 and 45 cm for those of the second order, while those of the third order were very close to the surface of the soil (0–15 cm). Most of the roots of the olive tree are located under the tree crown (Masmoudi-Charfi et al., 2011), as the olive tree establishes a balance between the roots and the crown. The further we move away from the canopy area, the lower the root density becomes. In this case, and in the middle of the rows between the trees (4 m away from the trunk), olive roots have been described as generally < 2 mm in diameter (fine and very fine) and few from 2 to 5 mm (medium) in the first 49 cm, although limited by a calcareous crust (Ckm horizon, 49–51 cm; Table 1). It is generally accepted that in areas with petrocalcic horizons, the olive tree roots under the canopy, break through the calcareous crust in order to have a greater anchorage and soil volume where it can obtain water and nutrients (Fan et al., 2017), blurring the

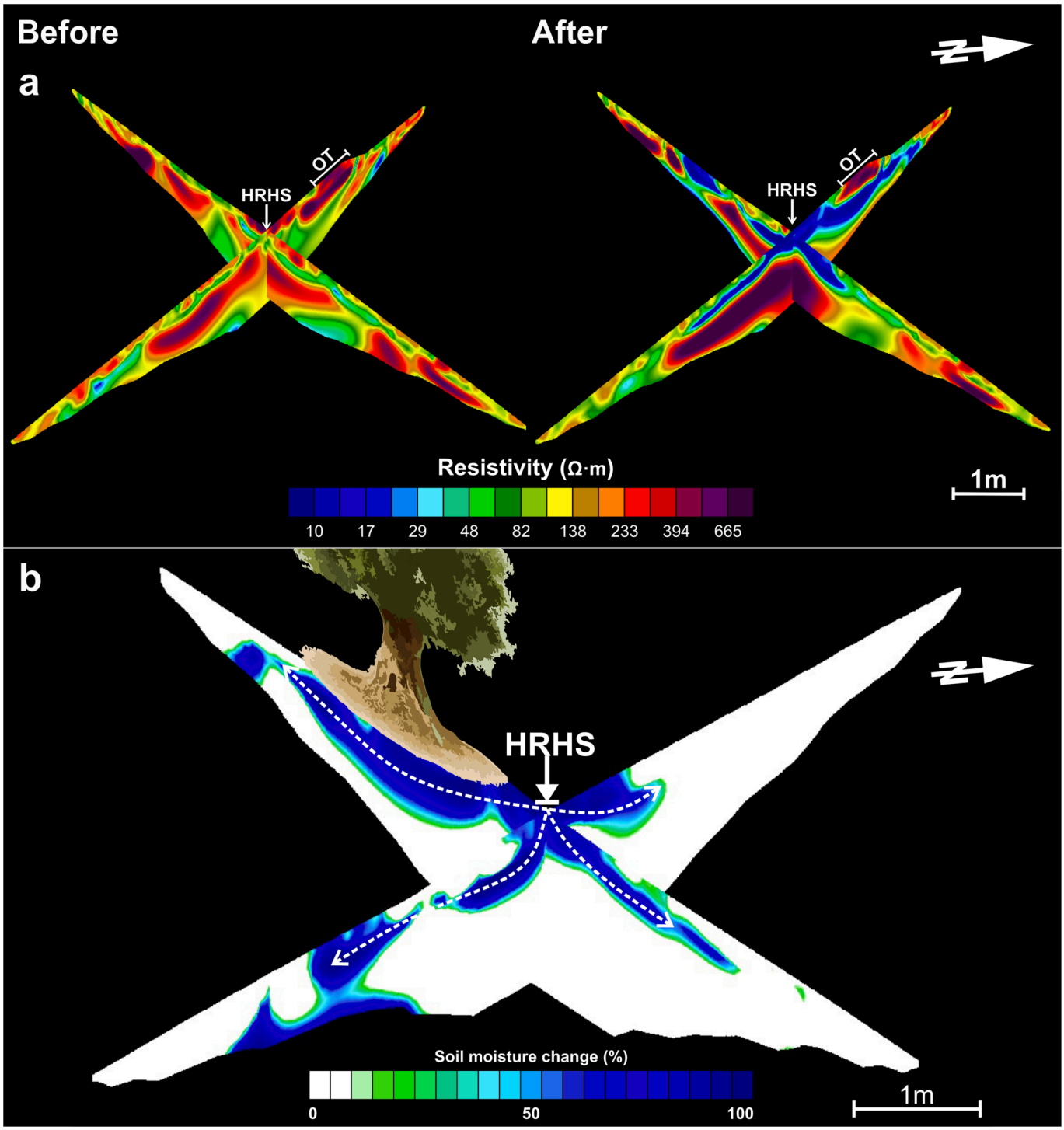

Fig. 8. 3D view of the ERT profiles. (a) Resistivity distribution of the profiles measured before (left) and after (right) rainfall simulation. (b) Change in soil moisture in percent after rain simulation. The blue zone shows the area with a 100% change in soil moisture, calculated from the ERT profiles in time-lapse. HRHS: Hydroinfiltrator Rainwater Harvesting System. OT: Position of the olive tree.

soil profile.

There are numerous pores –many of them biopores– in the root zone of the olive tree. According to Colombi et al. (2017), roots prefer to use the existing macropores and their interconnections to grow and thus cross soil zones with greater mechanical resistance. Roots influence the soil surrounding them by exerting pressure on it as they grow, reducing porosity in soil-root contact (Bengough, 2003; Lucas et al., 2019), creating more stable biopore walls (bathtub effect).

The emergence of preferential pathways is mainly due to two processes. The first is that during periods of water deficit, the mortality of fine roots increases, even in irrigated olive trees (Masmoudi-Charfi et al., 2011). These dead roots form biopores connected to the rest of the olive tree's roots through which water can circulate. The second process is related to the plant's water stress: The root shrinks (essentially the bark cells), significantly reducing the contact between the root and the soil (Weil and Brady, 2017; Logsdon, 2013). This gap between the soil and the root is beneficial because: 1) it reduces water loss from the root to the dry soil, although some of these roots die due to water stress; 2)

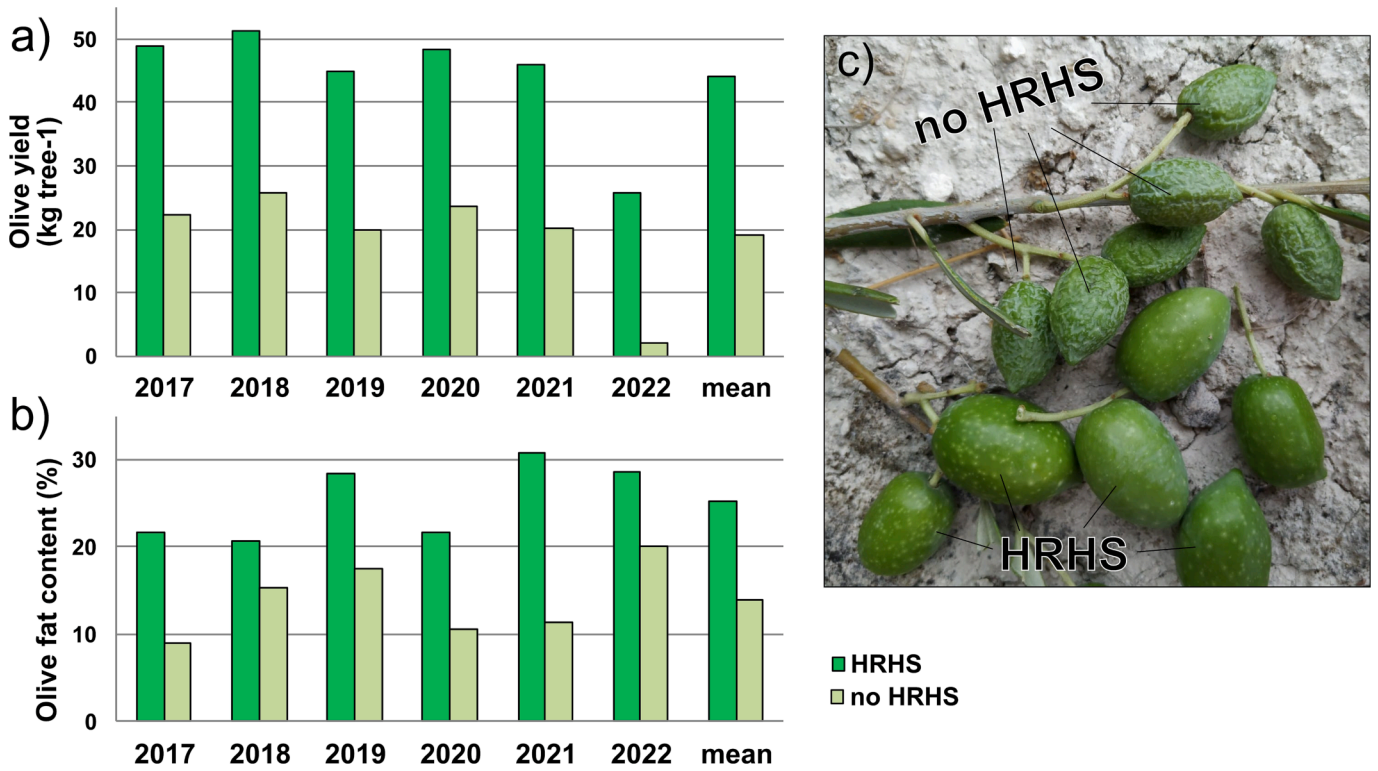

Fig. 9. Impact of HRHS on field performance of olive trees cultivated on hillslopes. Olive production (a) and fat yield (b) from 2017 to 2022 seasons with and without HRHS devices. (c) Effect of HRHS on size of olive fruits variety "Picuda".

this gap creates a preferential pathway for water to enter the soil. In summary, the root system of the olive tree is configured in an interconnected porous system, which we identify as the preferred pathways for water circulation. This would explain why the greatest amount of water detected in the ERT profiles is found under the canopy (around the roots of the boot) and in areas farther away from the trunk where greater root development occurs (Figs. 6 and 7). The fact that the soil aggregates in the root zone of the olive tree, and is very stable, also contributes to the effectiveness of these preferred routes, as the combination of roots, fungi and bacteria plays an important role in their formation (Logsdon, 2013). This water stability of the aggregates keeps the preferential pathways between the aggregates open.

4.3. Soil moisture distribution in the subsoil as a result of a HRHS

The model flow calculated for a standard study case and fitted to the soil properties shows that the groundwater distribution infiltrated by the *HRHS* has gravitational flows to depth (Fig. 6). However, the resistivity profiles indicate that the water remains in the first 50 cm of depth, which is consistent with the location of the thin calcareous crust acting as an impermeable barrier at this depth (Figs. 7 and 8). In addition, they suggest that in the area below the olive trunk, where the roots break through the calcareous layer, the water infiltrates to a slightly greater depth.

The model flow does not consider the preferred pathways created by the roots, as explained above, and in general these models are not applicable for these cases. In the model of percentage change in humidity calculated from the ERT time-lapse profiles, it can be observed that around the roots, the percentage change in humidity increases up to 100%, while the surrounding areas remain unchanged (Fig. 8b). The profiles were measured during a period of water deficit (August 2020), consequently the pathways created by the roots are the preferred areas for water flow at this time, as opposed to gravitational flow as indicated in the simplified model flow.

4.4. Benefits of the HRHS

Masmoudi-Charfi et al. (2011) notes that the highest root density (0.5 cm cm^{-3}) is found 40 cm from the trunk of young olive trees and that this density decreases with increasing distance from the trunk. Outside the zone under the crown, the presence of roots is very scarce. Therefore, the location of the *HRHS* near the trunk (upstream) and the vertical dimension of the device itself (40 cm into the ground) are ideal. In this way, the *HRHS* connects the outdoor area with the area of maximum root density, *i.e.* it connects the outdoor area with the system of preferred paths created by the rooting of the olive tree. In this way, the water that penetrates through the device can reach the most distant roots of the tree. This means that the water is stored in the root zone of the tree and not on the surface, thus avoiding evaporation due to high temperatures.

This mode of action of the *HRHS* (Delgado et al., 2019), which is considered to be vertical mulching in the sense of Ilha et al. (2021), makes it a good method to support other traditional methods and systems of rainwater harvesting in rainfed tree groves, as they have significant limitations (Mekdaschi-Studer and Liniger, 2013; Ammar et al. 2016). In endorheic micro-catchments, for example, the main limitation is the formation of superficial depositional crusts with little or no infiltration capacity (low infiltration velocity) in the lower part of the microbasin (Valentin and Bresson, 1992). Placing the hydroinfiltrator at this point solves this problem and breaks the barrier of scab formation.

Surface drip irrigation is relatively ineffective, as the water is subjected to a high evaporation rate from the surface moisture zone that occurs around each drip (mainly in semi-arid regions), which can be as high as 44% (Matthias et al., 1986; Lucero-Vega et al., 2017). To reduce such evaporation rates, Meshkat et al. (2000) and Mostafa (2014) suggested placing the dripper directly above a sand tube or vertical (compost) mulch (they removed a core of soil and replaced it with an equal volume of sand or compost, which is responsible for transferring water to the soil through vertical and horizontal flow). This is the same

effect that the *HRHS* achieves in agricultural soils with drip irrigation systems.

This is particularly interesting in deficit irrigation [applying water below the full water requirement of the crop; Fereres and Soriano (2007)], as the *HRHS* optimises the amount of water used. By avoiding water loss through direct evaporation - which is greater in the middle of the day - the *HRHS* maximises production per unit of water used (water productivity).

Further benefits come from the main component of the harvesting system: biochar. Although it is only present at the site where the unit is located, this material increases saturated and unsaturated hydraulic conductivity (Ajayi and Horn, 2016; Blanco-Canqui, 2017), increases soil water-holding capacity (Liu et al., 2016; Zhou et al., 2019), sequesters atmospheric carbon (Brassard et al., 2016), and increases soil fertility (Ding et al., 2016), among other effects.

Ilha et al. (2021) predict a reduction in water erosion and an enrichment of the water table for places where vertical mulching systems are installed (where the *HRHS* is included). For the latter, we can make some simple calculations for the case of our experimental plot. Rain falling into the 64 m^2 of the micro-basin would percolate through the *HRHS* and form a 3 × 5 m moisture island with surface projection (as suggested by the ERT images (Figs. 6 and 7). Under these conditions, a moisture island would form that could hold 1800 L of usable water. Assuming 100% system efficiency, this amount of water would be reached in a storm of 28.13 mm. With this amount of precipitation, excess water –gravitational water– would percolate towards the water table.

These results support the most positive final consequence of the HRHS which is the increase in olive production. As shown in Fig. 9, the olive trees with the device increased their production and fat yield of olives by 177% (production) and 211% (yield) respectively. Keeping in mind that the devices were installed in 2016, the increase in production since the first season has been remarkable (2017). This has very positive implications for a future where climate change is leading to a decrease in rainfall and an increase in evapotranspiration, resulting in a decrease in overall olive production in the Mediterranean region.

Finally, it is worth highlighting that this work is the first evaluation of the performance of olive trees growing in marginal areas, showing the differences between rainfed trees with and without the hydroinfiltrator system. The most significant finding being that in the treatment increased yield and fruit size, as well as exerting a positive effect on fruit development and fat oil accumulation (Fig. 9). Therefore, further studies are to be carried out to study the effect of *HRHS* devices on the ripening evolution of the olive fruit variety “Picuda” as well as the composition and total quality of the yield including sensorial evaluation of the resulting oils.

5. Concluding remarks and future perspectives

The new infiltration device (ES Patent No.: ES2793448 B2) has proven to be an effective tool in mitigating the adverse effects of water shortage scenarios for hillslope farming of woody fruit trees, which is being aggravated by climate change. Their use can be addressed in the FAO’s climate-smart agriculture concept: help farmers build strategies to adapt to climate change, sustainably increase agricultural production, and reduce greenhouse gasses (biochar sequesters carbon in the soil). By using electrical resistivity tomography and soil moisture analysis, we have proven that the new infiltration device: (i) increases moisture in the soil endopedons (so reduced evaporation); (ii) aids in the retention of water in the root zone of the olive tree (the excess water could recharge of the aquifers by percolation); and (iii) increases the olive yield and quality. Moreover, the hydroinfiltrator has a positive impact on the effects of torrential rains because the surface runoff could be intercepted by the device, reducing the intensity of water erosion process for hillslopes in Mediterranean semiarid environments.

Against this background, future research will go in the following directions: first, further study is needed on how the roots of the plants distribute and develop over time after the implantation of the infiltration device, as the roots have a positive tropism for water, thus, presumably the roots will develop more towards the moist areas near the infiltration device. Secondly, further research is needed with other soil types as well as with other rainfed woody fruit trees (almonds, pistachios, vineyards, etc.), particularly in Mediterranean marginal agricultural areas in combination with other standard strategies such as agricultural techniques that focus on conservation (plant covers, no-till, minimum tillage, etc.).

Ultimately, the impact of this type of adapted rainfed olive orchard with a *HRHS* system, besides aiding in the the increase in production and enabling changes in farming methods, could have important socioeconomic and environmental repercussions, and thus enable the agricultural sector to increase its competitiveness.

Declaration of Competing Interest

The authors declare that they have no known competing financial interests or personal relationships that could have appeared to influence the work reported in this paper.

Data availability

Data will be made available on request.

Acknowledgements

We would like to acknowledge the company Hydroinfiltrador S.L. for their support in conducting the research on their experimental plot. Furthermore, we would like to thank the two anonymous reviewers for their suggestions that improved the article.

References

Abhilash Joseph, E., Abdul Hakkim, V.M., Sajeena, S., 2020. Precision Farming for Sustainable Agriculture. International Journal of Agriculture Innovations and Research 8 (16), 543–553.

Ajayi, A.E., Horn, R., 2016. Modification of chemical and hydrophysical properties of two texturally differentiated soils due to varying magnitudes of added biochar. Soil and Tillage Research 164, 34–44. https://doi.org/10.1016/J.STILL.2016.01.011.

Al-Seekh, S.H., Mohammad, A.G., 2009. The effect of water harvesting techniques on runoff, sedimentation, and soil properties. Environmental Management 44 (1), 37–45. https://doi.org/10.1007/S00267-009-9310-Z/FIGURES/10.

Ammar, A., Riksen, M., Ouessar, M., Ritsema, C., 2016. Identification of suitable sites for rainwater harvesting structures in arid and semi-arid regions: A review. International Soil and Water Conservation Research 4 (2), 108–120. https://doi.org/10.1016/J.ISWCR.2016.03.001.

Beckers, B., Berking, J., Schütt, B., 2013. Ancient Water Harvesting Methods in the Drylands of the Mediterranean and Western Asia. Journal for Ancient Studies 2, 145–164. http://journal.topoi.org/index.php/etopoi/article/view/174.

Bengough, A.G., 2003. Root Growth and Function in Relation to Soil Structure, Composition, and Strength. In: de Kroon, H., Visser, E.J.W. (Eds.), Root Ecology. Springer, Berlin Heidelberg, Berlin, Heidelberg, pp. 151–171.

Blanco-Canqui, H., 2017. Biochar and Soil Physical Properties. Soil Science Society of America Journal 81 (4), 687–711. https://doi.org/10.2136/SSSAJ2017.01.0017.

Bongi, G., Palliotti, A., 1994. Olive. In: Schaffer, B., Andresen, P. (Eds.), Handbook of environmental physiology of fruit crops. CRC Press, pp. 165–187.

Brassard, P., Godbout, S., Raghavan, V., 2016. Soil biochar amendment as a climate change mitigation tool: Key parameters and mechanisms involved. Journal of Environmental Management 181, 484–497. https://doi.org/10.1016/J.JENVMAN.2016.06.063.

Cárceles Rodríguez, .B., Durán, Zuazo, V.H., Soriano, R.M., Gálvez, R.B., García T.I.F., 2021. Soil erosion and the effectiveness of the conservation measures in Mediterranean hillslope farming (SE Spain). Eurasian Soil Science 54, 792–806. https://doi.org/10.1134/S1064229321050069.

Colombi, T., Braun, S., Keller, T., Walter, A., 2017. Artificial macropores attract crop roots and enhance plant productivity on compacted soils. Science of The Total Environment 574, 1283–1293. https://doi.org/10.1016/J.SCITOTENV.2016.07.194.

Connor, D.J., Fereres, E., 2004. The Physiology of Adaptation and Yield Expression in Olive. Horticultural Reviews. John Wiley & Sons Inc, Oxford, UK, pp. 155–229.

Costagli, G., Gucci, R., Rapoport, H., 2003. Growth and development of fruits of olive ‘Frantoio’ under irrigated and rain-fed conditions. Journal of Horticultural Science

and Biotechnology 78 (1), 119–124. https://doi.org/10.1080/14620316.2003.11511577.
Junta de Andalucía, 2022. Red de Información Agroclimática de Andalucía (RIA). https://www.juntadeandalucia.es/agriculturaypesca/ifapa/riaweb/web/.
Delgado, G., Martín-García, J.M., Rojano-Cruz, R., Rufian, J.A., 2019. Dispositivo Infiltrador (Spain Patent No. ES 2 793 448 A1). Oficina Española de Patentes y Marcas. https://consultas2.oepm.es/pdf//ES/0000/000/02/79/34/ES-2793448_A1.pdf.
Delgado, J.A., Nearing, M.A., Rice, C.W., 2013. Chapter Two - Conservation Practices for Climate Change Adaptation. In: Sparks, D.L. (Ed.), Advances in Agronomy, Vol 121. Academic Press, pp. 47–115. https://doi.org/10.1016/B978-0-12-407685-3.00002-5.
Deng, S., Yin, Q., Zhang, S., Shi, K., Jia, Z., Ma, L., 2017. Drip Irrigation Affects the Morphology and Distribution of Olive Roots. HortScience 52 (9), 1298–1306. https://doi.org/10.21273/HORTSCI11997-17.
Ding, Y., Liu, Y., Liu, S., Li, Z., Tan, X., Huang, X., Zeng, G., Zhou, L., Zheng, B., 2016. Biochar to improve soil fertility. A review. Agronomy for Sustainable Development 36 (2), 1–18. https://doi.org/10.1007/S13593-016-0372-Z.
Durán Zuazo, V.H., Rodríguez Pleguezuelo, C.R., Arroyo Panadero, L., Martínez Raya, A., Francia Martínez, J.R., Cárceles Rodríguez, B., 2009. Soil Conservation Measures in Rainfed Olive Orchards in South-Eastern Spain: Impacts of Plant Strips on Soil Water Dynamics. Pedosphere 19 (4), 453–464. https://doi.org/10.1016/S1002-0160(09)60138-7.
El Riachy, M., Haber, A., Daya, S.A., Jebbawi, G., Al Hawi, G., Talej, V., Houssein, M., El Hajj, A., P., 2017. Influence of irrigation regimes on quality attributes of olive oils from two varieties growing in Lebanon. International Journal of Environment Agriculture and Biotechnology 2 (2), 895–905. https://doi.org/10.22161/ijeab/2.2.43.
El-Nashar, W., Elyamany, A., 2023. Adapting irrigation strategies to mitigate climate change impacts: a value engineering approach. Water Resource Management 37, 2369–2386. https://doi.org/10.1007/s11269-022-03353-4.
Fan, Y., Miguez-Macho, G., Jobbágy, E.G., Jackson, R.B., Otero-Casal, C., 2017. Hydrologic regulation of plant rooting depth. Proceedings of the National Academy of Sciences of the United States of America 114 (40), 10572–10577. https://doi.org/10.1073/PNAS.1712381114/-DCSUPPLEMENTAL.
Fao, 2014. Compendium on Rainwater Harvesting for Agriculture in the Caribbean Sub-region. Concepts, calculations and definitions for small, rain-fed farm systems. accessed at 11 Feb 2021 Technical Report. Available at. http://www.fao.org/3/a-br326e.pdf.
Fereres, E., 1984. Variability in adaptive mechanisms to water deficits in annual and perennial crop plants. Bull. Soc. Bot. Fr. 131, 17–32. https://doi.org/10.1080/01811789.1984.10826629.
Fereres, E., Soriano, M.A., 2007. Deficit irrigation for reducing agricultural water use. Journal of Experimental Botany 58 (2), 147–159. https://doi.org/10.1093/jxb/erl165.
Fernández, J.E., Moreno, F., Girón, I., Blázquez, O.M., 1997. Stomatal control of water use in olive tree leaves. Plant and Soil 190, 179–192. https://doi.org/10.1023/A:1004293026973.
Ferreira, C.S.S., Seifollahi-Aghmiuni, S., Destouni, G., Ghajarnia, N., Kalantari, Z., 2022. Soil degradation in the European Mediterranean region: Processes, status and consequences. Science of The Total Environment 805, 150106. https://doi.org/10.1016/j.scitotenv.2021.150106.
Fraga, H., Moriondo, M., Leolini, L., Santos, J.A., 2021. Mediterranean Olive Orchards under Climate Change: A Review of Future Impacts and Adaptation Strategies. Agronomy 11 (1), 56. https://doi.org/10.3390/agronomy11010056.
Freihat, N.M., Shannag, H.K., Alkelani, M.A., 2021. Effects of supplementary irrigation on performance of 'Nabali' and 'Grossa de Spain' olives under semi-arid conditions in Jordan. Scientia Horticulturae 275, 109696. https://doi.org/10.1016/j.scienta.2020.109696.
Funes, I., Savé, R., de Herralde, F., Biel, C., Pla, E., Pascual, D., Zabalza, J., Cantos, G., Borràs, G., Vayreda, J., Aranda, X., 2021. Modeling impacts of climate change on the water needs and growing cycle of crops in three Mediterranean basins. Agricultural Water Management 249, 106797. https://doi.org/10.1016/J.AGWAT.2021.106797.
García-Ruiz, J.M., López-Moreno, I.I., Vicente-Serrano, S.M., Lasanta-Martínez, T., Beguería, S., 2011. Mediterranean water resources in a global change scenario. Earth-Science Reviews 105 (3–4), 121–139. https://doi.org/10.1016/J.EARSCIREV.2011.01.006.
Giorgi, F., Lionello, P., 2008. Climate change projections for the Mediterranean region. Global and Planetary Change 63 (2–3), 90–104. https://doi.org/10.1016/J.GLOPLACHA.2007.09.005.
Gómez, R.A., Salvador, M.D., Moriana, A., Pérez, D., Olmedilla, N., Ribas, F., Fregapane, G., 2007. Influence of different irrigation strategies in a traditional Cornicabra cv. Olive orchard on virgin olive oil composition and quality". Food Chemistry 100, 568–578. https://doi.org/10.1016/j.foodchem.2005.09.075.
Gosling, S.N., Arnell, N.W., 2016. A global assessment of the impact of climate change on water scarcity. Climate Change 134, 371–385. https://doi.org/10.1007/s10584-013-0853-x.
Goubanova, K., Li, L., 2007. Extremes in temperature and precipitation around the Mediterranean basin in an ensemble of future climate scenario simulations. Global and Planetary Change 57 (1–2), 27–42. https://doi.org/10.1016/J.GLOPLACHA.2006.11.012.
Hoerling, M., Eischeid, J., Perlwitz, J., Quan, X., Zhang, T., Pegion, P., 2012. On the Increased Frequency of Mediterranean Drought. Journal of Climate 25 (6), 2146–2161. https://doi.org/10.1175/JCLI-D-11-00296.1.
Iglesias, A., Garrote, L., Flores, F., Moneo, M., 2007. Challenges to manage the risk of water scarcity and climate change in the Mediterranean. Water Resources Management 21, 775–788. https://doi.org/10.1007/s11269-006-9111-6.
Ilha, R., de Paiva, J.B.D., Righes, A.A., Borg, H., 2021. A method to compute the effect of vertical mulching on the reduction of surface runoff. Environmental Monitoring and Assessment 193, 1–19. https://doi.org/10.1007/s10661-021-09509-w.
Inglese, P., Barone, E., Gullo, G., 1996. The effect of complementary irrigation on fruit growth, ripening pattern and oil characteristics of olive (*Olea europaea* L.) cv. Carolea. Journal of Horticultural Science 71 (2), 257–263. https://doi.org/10.1080/14620316.1996.11515404.
IUSS Working Group WRB, 2014. World Reference Base for Soil Resources 2014. International soil classification system for naming soils and creating legends for soil maps. World Soil Resources Reports No. 106. FAO, Rome.
Jiménez, M.A., Izquierdo, E., Rodríguez, F., Dueñas, J.I., Tortosa, C., 2000. Determinación de grasa y humedad en aceitunas mediante medidas de reflectancia en infrarrojo cercano. Grasas y Aceites 51 (5), 311–315.
Kumar, D., Ahmed, N., Srivastava, K.K., Singh, S.R., Hassan, A., 2013. Micro-catchment water harvesting and moisture conservation techniques for apple (Malus domestica) production under rainfed condition. Indian Journal of Agricultural Sciences 83 (12), 46–50.
Kumar, S., Meena, R.S., Jakhar, S.R., Jangir, C.K., Gupta, A., Meena, B.L., 2019. Adaptation strategies for enhancing agricultural and environmental sustainability under current climate. Sustainable agriculture. Scientific Publisher, Jodhpur, 226-274. ISBN : 978-93-88043-62-5.
Li, M., Liu, T., Duan, L., Luo, Y., Ma, L., Zhang, J., Zhou, Y., Chen, Z., 2019. The scale effect of double-ring infiltration and soil infiltration zoning in a semi-arid steppe. Water 11 (7), 1457. https://doi.org/10.3390/W11071457.
Liu, C., Wang, H., Tang, X., Guan, Z., Reid, B.J., Rajapaksha, A.U., Ok, Y.S., Sun, H., 2016. Biochar increased water holding capacity but accelerated organic carbon leaching from a sloping farmland soil in China. Environmental Science and Pollution Research 23, 995–1006. https://doi.org/10.1007/s11356-015-4885-9.
Lodolini, E.M., Polverigiani, S., Ali, S., Mutawea, M., Qutub, M., Pierini, F., Neri, D., 2016. Effect of complementary irrigation on yield components and alternate bearing of a traditional olive orchard in semi-arid conditions. Spanish Journal of Agricultural Research 14 (2). https://doi.org/10.5424/sjar/2016142-8834.
Logsdon, S.D., 2013. Root effects on soil properties and processes: synthesis and future research needs. enhancing understanding and quantification of soil–root growth interactions. In: Ahuja, Timlin y L.R. (Ed.), Advances in Agricultural Systems Modeling, 4, pp. 173–196. https://doi.org/10.2134/advagricsystmodel4.c8.
Loke, M.H., 2022. Tutorial: 2-D and 3-D electrical imaging surveys.
Lorite, I.J., Gabaldón-Leal, C., Ruiz-Ramos, M., Belaj, A., de la Rosa, R., León, L., Santos, C., 2018. Evaluation of olive response and adaptation strategies to climate change under semi-arid conditions. Agricultural Water Management 204, 247–261. https://doi.org/10.1016/J.AGWAT.2018.04.008.
Lucas, M., Schlüter, S., Vogel, H.J., Vetterlein, D., 2019. Roots compact the surrounding soil depending on the structures they encounter. Scientific Reports 9 (1), 1–13. https://doi.org/10.1038/s41598-019-52665-w.
Lucero-Vega, G., Troyo-Diéguez, E., Murillo-Amador, B., Nieto-Garibay, A., Ruíz-Espinoza, F.H., Beltrán-Morañes, F.A., Zamora-Salgado, S., 2017. Diseño de un sistema de riego subterráneo para abatir la evaporación en suelo desnudo comparado con dos métodos convencionales. Agrociencia 51(5), 487-505. ISSN 2521-9766.
Martínez-Martos, M., Galindo-Zaldívar, J., Sanz de Galdeano, C., García-Tortosa, F.J., Martínez-Moreno, F.J., Ruano, P., González-Castillo, L., Azañón, J.M., 2017. Latest extension of the Laujar fault in a convergence setting (Sierra Nevada, Betic Cordillera). Journal of Geodynamics 104, 15–26. https://doi.org/10.1016/J.JOG.2016.12.002.
Martínez-Moreno, F.J., Galindo-Zaldívar, J., Pedrera, A., González-Castillo, L., Ruano, P., Calaforra, J.M., Guirado, E., 2015. Detecting gypsum caves with microgravity and ERT under soil water content variations (Sorbas, SE Spain). Engineering Geology 193, 38–48. https://doi.org/10.1016/J.ENGGEO.2015.04.011.
Martos-Rosillo, S., Ruiz-Constán, A., González-Ramón, A., Mediavilla, R., Martín-Civantos, J.M., Martínez-Moreno, F.J., Jódar, J., Marín-Lechado, C., Medialdea, A., Galindo-Zaldívar, J., Pedrera, A., Durán, J.J., 2019. The oldest managed aquifer recharge system in Europe: New insights from the Espino recharge channel (Sierra Nevada, southern Spain). Journal of Hydrology 578.
Masmoudi-Charfi, C., Masmoudi, M., Ben Mechlia, N., 2011. Root distribution in young Chétoui olive trees (*Olea europaea* L.) and agronomic applications. Advances in Horticultural Science 25, 112–122. https://doi.org/10.13128/ahs-12776.
Matthias, A.D., Salehi, R., Warrick, A.W., 1986. Bare soil evaporation near a surface point-source emitter. Agricultural Water Management 11 (3), 257–277. https://doi.org/10.1016/0378-3774(86)90043-0.
Mekdaschi-Studer, R., Liniger, H., 2013. Water Harvesting: Guidelines to Good Practice. Centre for Development and Environment (CDE), Bern; Rainwater Harvesting Implementation Network (RAIN), Amsterdam; MetaMeta, Wageningen; The International Fund for Agricultural Development (IFAD), Rome.
Meshkat, M., Warner, R.C., Workman, S.R., 2000. Evaporation reduction potential in an undisturbed soil irrigated with surface drip and sand tube irrigation. Transactions of the ASAE 43 (1), 79–86.
Mostafa, H.M.S., 2014. Effective moisture conservation method for heavy soil under drip irrigation. Agricultural Engineering International: CIGR Journal 16 (2), 1–9.
Palese, A.M., Vignozzi, N., Celano, G., Agnelli, A.E., Pagliai, M., Xiloyannis, C., 2014. Influence of soil management on soil physical characteristics and water storage in a mature rainfed olive orchard. Soil and Tillage Research 144, 96–109. https://doi.org/10.1016/J.STILL.2014.07.010.
Rodrigo-Comino, J., Senciales, G.J.M., Yu, Y., Salvati, L., Giménez, A.M., Cerda, A., 2021. Long-term changes in rainfed olive production, rainfall and farmer's income in

Bailén (Jaén, Spain). Euro-Mediterranean Journal for Environmental Integration 6, 58. https://doi.org/10.1007/s41207-021-00268-1.

Slate, M.L., Durham, R.A., Casper, C., Mummey, D., Ramsey, P., Pearson, D.E., 2023. No evidence of three herbicides and one surfactant impacting biological soil crusts. Restoration Ecology e13802. https://doi.org/10.1111/rec.13802.

Soil Survey Staff, 1999. Soil taxonomy: a basic system of soil classification for making and interpreting soil surveys, 2nd edition. Agriculture handbook. Soil Conservation Service, US Department of Agriculture, United States Department of Agriculture, Natural Resources Conservation Service.

Soil Survey Staff, 2014. Keys to soil taxonomy, 12th edition. Washington, DC, USA, United States Department of Agriculture.

Sorgonà, A., Proto, A.R., Abenavoli, L.M., Iorio, A.D., 2018. Spatial distribution of coarse root biomass and carbon in a high-density olive orchard: effects of mechanical harvesting methods. Trees 32, 919–931. https://doi.org/10.1007/s00468-018-1686-z.

Tadros, M.J., Al-Mefleh, N.K., Othman, Y.A., Al-Assaf, A., 2021. Water harvesting techniques for improving soil water content, and morpho-physiology of pistachio trees under rainfed conditions. Agricultural Water Management 243, 106464. https://doi.org/10.1016/J.AGWAT.2020.106464.

Tanasijevic, L., Todorovic, M., Pereira, L.S., Pizzigalli, C., Lionello, P., 2014. Impacts of climate change on olive crop evapotranspiration and irrigation requirements in the Mediterranean region. Agricultural Water Management 144, 54–68. https://doi.org/10.1016/J.AGWAT.2014.05.019.

Trabelsi, L., Gargouri, K., Ayadi, M., Mbadra, C., Ben Nasr, M., Ben Mbarek, H., Ghrab, M., Ben Ahmed, G., Kammoun, Y., Loukil, E., Maktouf, S., Khlifi, M., Gargouri, R., 2022. Impact of drought and salinity on olive potential yield, oil and fruit qualities (cv. Chemlali) in an arid climate. Agricultural Water Management 269. https://doi.org/10.1016/j.agwat.2022.107726.

Tubeileh, A., Bruggeman, A., Turkelboom, F., 2009. Effect of water harvesting on growth of young olive trees in degraded Syrian dryland. Environment, Development and Sustainability 11 (5), 1073–1090. https://doi.org/10.1007/S10668-008-9167-Y/FIGURES/9.

Tubeileh, A., Bruggeman, A., Turkelboom, F., 2016. Water-harvesting designs for fruit tree production in dry environments. Agricultural Water Management 165, 190–197. https://doi.org/10.1016/J.AGWAT.2015.11.006.

Valentin, C., Bresson, L.M., 1992. Morphology, genesis and classification of surface crusts in loamy and sandy soils. Geoderma 55 (3–4), 225–245. https://doi.org/10.1016/0016-7061(92)90085-L.

Valverde, P., de Carvalho, M., Serralheiro, R., Maia, R., Ramos, V., Oliveira, B., 2015. Climate change impacts on rainfed agriculture in the Guadiana river basin (Portugal). Agricultural Water Management 150, 35–45. https://doi.org/10.1016/J.AGWAT.2014.11.008.

Weil, R.R., Brady, N.C., 2017. The nature and properties of soils, global edition. Pearson Education, Harlow.

Zhang, W., Sheng, J., Li, Z., Weindorf, D.C., Hu, G., Xuan, J., Zhao, H., 2021. Integrating rainwater harvesting and drip irrigation for water use efficiency improvements in apple orchards of northwest China. Scientia Horticulturae 275, 109728. https://doi.org/10.1016/J.SCIENTA.2020.109728.

Zhou, H., Fang, H., Zhang, Q., Wang, Q., Chen, C., Mooney, S.J., Peng, X., Du, Z., 2019. Biochar enhances soil hydraulic function but not soil aggregation in a sandy loam. European Journal of Soil Science 70 (2), 291–300. https://doi.org/10.1111/EJSS.12732.